Study of Temperature Effect on Far-Infrared Spectra of Liquid H_2O and D_2O by Analytical Theory and Molecular Dynamic Simulations

Alexander Y. Zasetsky

Department of Chemistry, University of Waterloo, Waterloo ON, N21 3GI, Canada

Vladimir I. Gaiduk*

Institute of Radio Engineering and Electronics, Russian Academy of Sciences, Vvedensky Sq. 1, Fryazino, 141190, Moscow Region, Russia

Received: March 5, 2007; In Final Form: April 18, 2007

The results of a combined study of dielectric loss ($\epsilon''(\nu)$) and power-absorption coefficient ($\alpha(\nu)$) are reported. The $\epsilon''(\nu)$ and $\alpha(\nu)$ values are obtained for liquid water (H_2O) and heavy water (D_2O) using analytical modeling and the molecular dynamics (MD) simulations method. The calculated spectra span the microwave and far-infrared (FIR) region. The temperature range probed is 220−355 K. Appropriate parametrization of the analytical model for liquid water enables the quantitative description of the dielectric spectra over the frequency range of 0−1000 cm^{-1}. An excellent agreement between the calculated spectra and the experimental data demonstrates the accuracy of the applied analytical approximations. The spectra obtained using the MD simulations agree rather qualitatively with the experimental $\epsilon''(\nu)$ and $\alpha(\nu)$ dependences. The observed spectra are interpreted in terms of four molecular mechanisms that have been recently described [*J. Phys. Chem. A* **2006**, *110,* 9361].

1. Introduction

A long-standing problem posed in the terahertz (THz) spectroscopy of liquid water and ice is to understand the molecular dynamics (MD) behind the absorption features in the microwave and far infrared (FIR) spectral regions. The problem is complicated by the fact that these regions are on a threshold between the primarily collective motion, observed at microwaves, and essentially intramolecular modes of the mid-infrared (mid-IR) region. It is becoming more and more evident that a quantitative description of the spectra for condensed H_2O phases in the FIR region requires a combination of these two very different-in-nature mechanisms (collective intermolecular and single-particle intramolecular) within a unified theory. Many aspects of the problem are not fully clear. A remarkable example is the 200 cm^{-1} band in liquid water and ice, the origin of which is still in dispute.[1]

The MD simulation technique can provide an insight, at a molecular level, into the motion mechanism of many interacting bodies. Even though this method has helped to achieve significant advances, especially with the development of the ab initio MD technique,[2] the understanding and interpretation of the MD responsible for microwave and FIR spectra (given, e.g., in ref 1 and refs 3−5) are not absolutely conclusive. In particular, the problem in the interpretation of the simulation results for the librational band at 700 cm^{-1} and especially for the translational band, centered at 200 cm^{-1}, has been encountered.[1−3]

On the other hand, considerable progress that has been made recently[6−10] in the analytical calculation of dielectric spectra for liquid water and ice (I_h) has enabled description of the autocorrelation function (ACF) spectra, in terms of the two-fraction model, based on application of effective potentials.

We believe that a combination of the MD technique, analytical models, and experimental data over a range of thermodynamic states can provide a new insight into the problem. To the best of our knowledge, a systematic comparison of the results of MD simulations (with classical potentials) with available experimental data for the condensed H_2O phases has not yet been performed in a systematic way. The results of molecular simulations also have not been accurately compared with the analytical calculations of such spectra. We shall correct these drawbacks in the present work. Namely, the MD simulations were partially performed over a range of temperatures, including those temperatures for which analytical calculations were reported earlier.[8] Within a chosen temperature interval, including the supercooled region, there exist the experimental data for liquid water.[11−14] We refer, in particular, to the work by Zelsmann,[14] where the data for the real and imaginary part of the complex refraction index are given in the wavenumber range of 19.5−600 cm^{-1}. In our previous work,[8] the results of analytical calculation of the dielectric spectra are compared with those from the work of Zelsmann.[14] For the comparison with the results of MD simulations, we also use the work of Liebe et al.,[15] where an empirical formula for the complex permittivity ($\epsilon(\nu)$) is suggested.

In section 2, we describe the simulation details and give a general outline of the results of this simulation. In section 3, the latter are compared with the experimental spectra. In section 4, a brief description of four molecular mechanisms, used in the analytical theory, is given. Section 5 presents the main result of our work, specifically the loss spectra of H_2O, obtained by MD simulations in the range of temperatures, which are compared with the spectra calculated analytically as well with available experimental data. The results of such a comparison are discussed in section 6.

10.1021/jp0717903 CCC: $37.00
Published on Web 06/07/2007

2. Molecular Dynamics (MD) Simulations

2.1. Calculation Details. In the present work, we use the extended simple point charge (SPC/E) model,[16] which is known to give reasonably accurate values of the static dielectric permittivity of liquid water under ambient conditions.[17] We performed the MD simulations for both water (H_2O) and heavy water (D_2O) with a system size of 1024 particles at temperatures of 220, 240, 267, 273, 300, and 355 K. The parallel MD code for arbitrary molecular mixtures (DynaMix, by Lyubartsev and Laaksonen[18]) is used. The simulations have been performed on a Linux cluster built on the Tyan/Opteron 64 platform, which enables calculations of relatively long trajectories for a system of 1024 water molecules. The simulation run lengths are dependent on temperature and are in the range of 1−4 ns for the warmest and coldest simulation, respectively. The initial condition was a cubic lattice; therefore, the equilibration time was chosen to be temperature-dependent in the range from 200 ps at 355 K to 1 ns at 200 K.

The motion equations have been solved using the Verlet Leapfrog algorithm, subject to periodic boundary conditions in a cubic simulation cell and a time step of 2 fs. The simulations have been performed in the NPT ensemble at atmospheric pressure (1 atm) with the Nose−Hoover thermostat.[19] The SHAKE constraints scheme[20] was used. We have used a spherical cutoff radius of 1.2 nm. The Ewald sum method was used to treat long-range electrostatic interactions.

For periodically replicated nonconducting molecular systems, the complex dielectric permittivity $\epsilon(\omega)$ can be computed from the time ACF of the total dipole moment[21] during the course of a simulation run as follows:

$$\frac{\epsilon(\nu) - n_\infty^{\,2}}{4\pi} = \frac{\langle \mathbf{M}^2 \rangle}{3Vk_BT}\left[1 + \int_0^\infty \mathrm{d}t e^{i\omega t}\frac{\partial C(t)}{\partial(t)}\right] \qquad (1)$$

with the complex refractive index n^* ($n^* = n + ik$) being given by

$$n^*(\nu) = \sqrt{\epsilon(\nu)} \qquad (2)$$

Here, $\epsilon(\nu)$ is the permittivity, with the complex conjugation symbol omitted ($\epsilon(\nu) = \epsilon'(\nu) + i\epsilon(\nu)$), n_∞ is the refractive index at infinite frequency, V is the volume of the simulation cell, k_B is the Boltzmann constant, and T is temperature. $\mathbf{M}$ is the total dipole moment of the simulation cell, where the angular brackets indicate the ensemble average. The dipole moment is computed as

$$\mathbf{M} = \sum_{i=1}^{N}\sum_{\alpha=1}^{3} \mathbf{r}_{i\alpha} q_\alpha \qquad (3)$$

where the summation runs over all the molecules (index i) and three atom sites (index α) carrying the charge value of q_α. $C(t)$ is the normalized ACF of the total dipole moment:

$$C(t) = \frac{\mathbf{M}(t)\mathbf{M}(0)}{\mathbf{M}^2(0)}$$

Note that we compute the function $C(t)$ and the value of the total dipole moment $\mathbf{M}$ independently, because sampling of the value $\mathbf{M}$ from trajectories generated by the MD method can be done much more often, which provides better statistics and, thus, more accurate value of the static dielectric constant ϵ_s, which is computed through the following relation:

$$\frac{\epsilon_s - n^2}{4\pi} = \frac{1}{3Vk_BT}(\langle \mathbf{M}^2 \rangle - \langle \mathbf{M} \rangle \langle \mathbf{M} \rangle) \qquad (4)$$

Velocity time ACFs $\langle \mathbf{v}(t)\mathbf{v}(0) \rangle$ for the center of mass (COM) of a water molecule have been computed in the local (molecular) coordinate frame, making it possible to look at the COM motion alone for each local (Cartesian) coordinate X, Y, and Z independently.[3] In the present work, all three atoms (O, H1, and H2) are placed on the $X0Z$ (molecular) plane and the H1−O−H2 median coincides with the Z-axis.

2.2. Spectral Density of Center-of-Mass (COM) Motion. We begin the discussion with the low-frequency end of the FIR region of 10−300 cm^{-1}. This region can, in part, be examined by the spectral intensity of the motion of molecular COM. Figure 1 shows the COM velocity ACFs for two temperatures: 220 and 352 K. Prominent variations in the COM motion with the changes in the direction and temperature are evident. The oscillation strength (magnitude) is noticeably larger at 220 K, in comparison to that at 235 K.

The spectral densities of the COM motion have two peaks, at ∼60 and ∼200 cm^{-1} (see Figure 2). The pronounced band at 60 cm^{-1} is not active in the IR region and has been recently attributed to the O−H bond bending [4] and earlier to the fluctuations of the dipole−induced dipole [3], which do not change the value of the total dipole moment. This implies that the mode is intermolecular in nature. The results of the present work show that it is still a subject for discussion, because the intense 60 cm^{-1} mode is observed in the simulations that use a rigid water molecule as a model.

The 200 cm^{-1} mode is active in the FIR spectrum of liquid water[11] and ice[22] and the Raman scattering spectra.[23] In a recent study[1] of the FIR spectrum of liquid D_2O by the Carr−Parrinello MD simulation method,[2] this mode is shown to result from intermolecular charge density fluctuations. The COM displacement is more probable in the Y-direction, perpendicular to the molecular plane; in contrast, it is diminished in the Z-direction, coincident with the *permanent* dipole moment of a water molecule.

In the classical simulations of the present work, the magnitude of the 200 cm^{-1} band increases as the temperature decreases. The COM motion of a water molecule is highly anisotropic, as shown in Figure 2, which illustrates the spectral density of the motion in the X-, Y-, and Z-directions, the latter of which being the most (intense) preferable at a wavenumber of 200−300 cm^{-1}. The exact position of this band is dependent on both temperature and direction. The mode magnitude is the largest for the motion in the Z-direction; it is centered at ∼250 cm^{-1} for the temperature of 325 K and at ∼270 cm^{-1} at 220 K. In the X-direction, the mode is located at ∼200 cm^{-1} at 325 K and it is shifted to a higher frequency of 220 cm^{-1} for supercooled water at 220 K. Some indication of the mode in the Y-direction does exist at ∼200 cm^{-1} in supercooled water at 220 K.

2.3. Spectra of the Total Dipole Moment Autocorrelation Function (ACF). The total dipole moment ACFs are shown in Figure 3. After initial fast decay due to molecular vibrations and reorientations (librations), which are observed at times of <0.1 ps, the total dipole moment ACFs exponentially decrease on the larger time scales. The slope of the exponential decays gives the dielectric relaxation time (see Table 1 for the exact values for the temperatures shown in Figure 3); the relaxation time ranges from ∼2 ps at 355 K to ∼25 ps at 267 K. The spectra of dielectric permittivity, $\epsilon(\nu) = \epsilon'(\nu) + i\epsilon(\nu)$, are computed using eq 1. In Figure 4, we illustrate the Cole−Cole

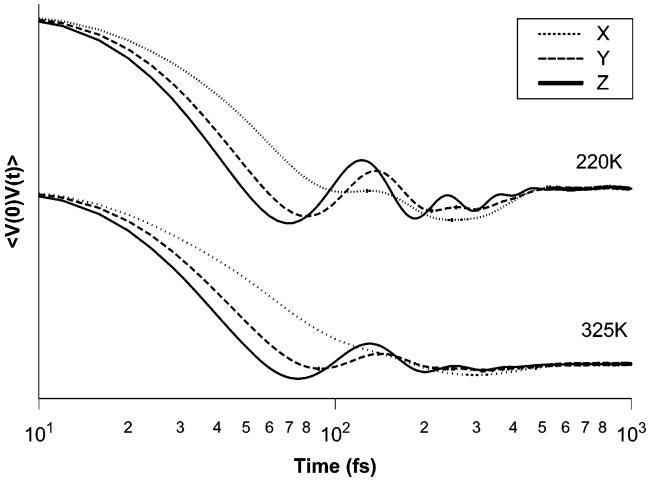

Figure 1. Velocity time autocorrelation functions (ACFs) of the center-of-mass (COM) in the local (molecular) coordinate frame for temperatures of 220 and 235 K.

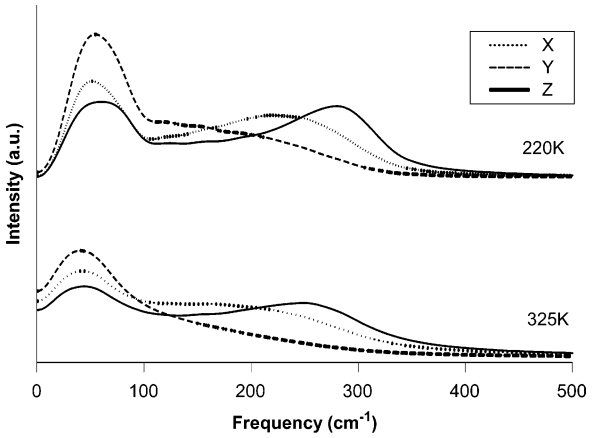

Figure 2. Spectral densities of the H_2O COM motion in the *X*-, *Y*-, and *Z*-directions for temperatures of 220 and 235 K.

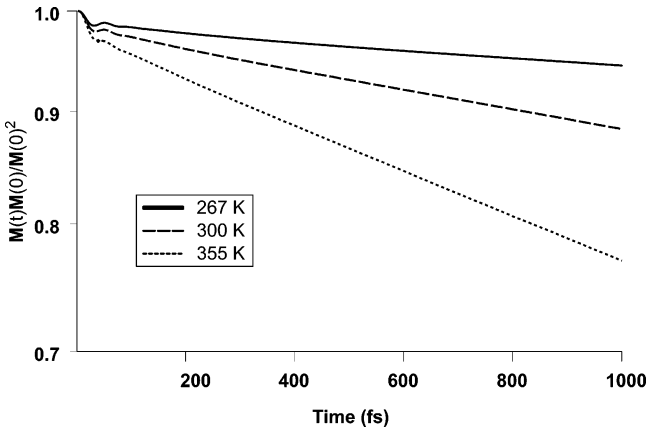

Figure 3. Total dipole moment determined by ACFs.

plot of the dielectric permittivity, $\epsilon''(\nu) = f[\epsilon'(\nu)]$, together with the spectra of the refractive indices (see eq 2) (shown in Figure 4b). The calculation results are summarized in Table 1. As might be expected, the MD simulations reveal a very strong temperature dependence of dielectric relaxation, which is reflected in the relaxation (Debye) time (τ_d); however, the peak position of the librational band—and, consequently, the librator's lifetime (τ_L)—is rather independent of temperature. The static dielectric permittivity (ϵ_s) decreases as the temperature decreases, and its value is in a good agreement with the earlier studies.[17]

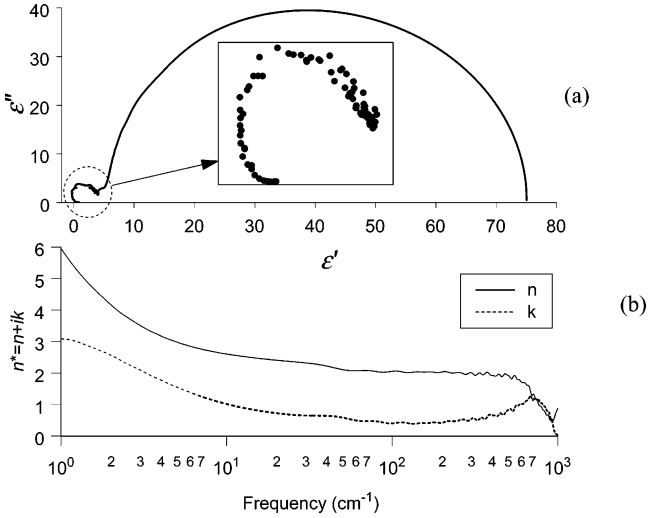

Figure 4. Refractive indices and Cole−Cole plot.

TABLE 1: Parameters Derived from MD Simulations with the Extended Simple Point Charge (SPC/E) Model

temperature, T (K)	ϵ_S	τ_d (ps)	f_L (cm^{-1})	τ_L (ps)
200	95	2320	775	0.0425
220	92	1050	779	0.0423
240	88	290	780	0.0423
267	80	25.3	781	0.0422
273	79	20.4	784	0.042
300	71	9.2	787	0.0419
355	57	4.2	783	0.042

3. Comparison with Experiment

In Figure 5a and b, we show the spectra of dielectric loss $\epsilon''(\nu)$ and the power absorption coefficient $\alpha(\nu)$, respectively, obtained from MD simulations at 300 K for liquid water (H_2O). In Figures 5c and 5d, the experimental spectra[14] observed for the same temperature are depicted by the solid lines and the spectra calculated from the empirical relationships[15] are shown by the dashed lines. The Debye loss peak (denoted as D) and librational mode peak (denoted as L) are observed in the microwave and FIR regions, respectively. These peaks agree correspondingly with the peaks in Figures 5a and 5b that were obtained by the MD simulations.

Figure 6 shows that the same agreement also holds at a temperature of 273 K. As expected, the decrease in temperature produces a significant shift of the dielectric loss peak D to lower frequencies.

In Figures 7a and b, we show the simulation results for heavy water (D_2O) at 273 K. The corresponding experimental spectra are shown in Figures 7c and d. The increase in the inertia moment of the water molecule results in a shift of the librational mode toward lower frequencies. Such temperature dependence agrees with the experimental results.

Figures 5−7 suggest that, for both temperatures (300 and 273 K), and for both water isotopes (H_2O and D_2O), the translation band, which generally arises at $\nu \approx 200$ cm^{-1}, is *not* observed in the spectra that are computed by the MD simulations (the latter give the spectra with an account of the total dipole moment determined by the calculated ACFs). In contrast, the translational-band peak, marked as T in the figures (see Figures 5−7) appears in the experimental spectra or in those spectra calculated from the empirical formulas.[15] We discuss a possible reason for this MD result in section 6.

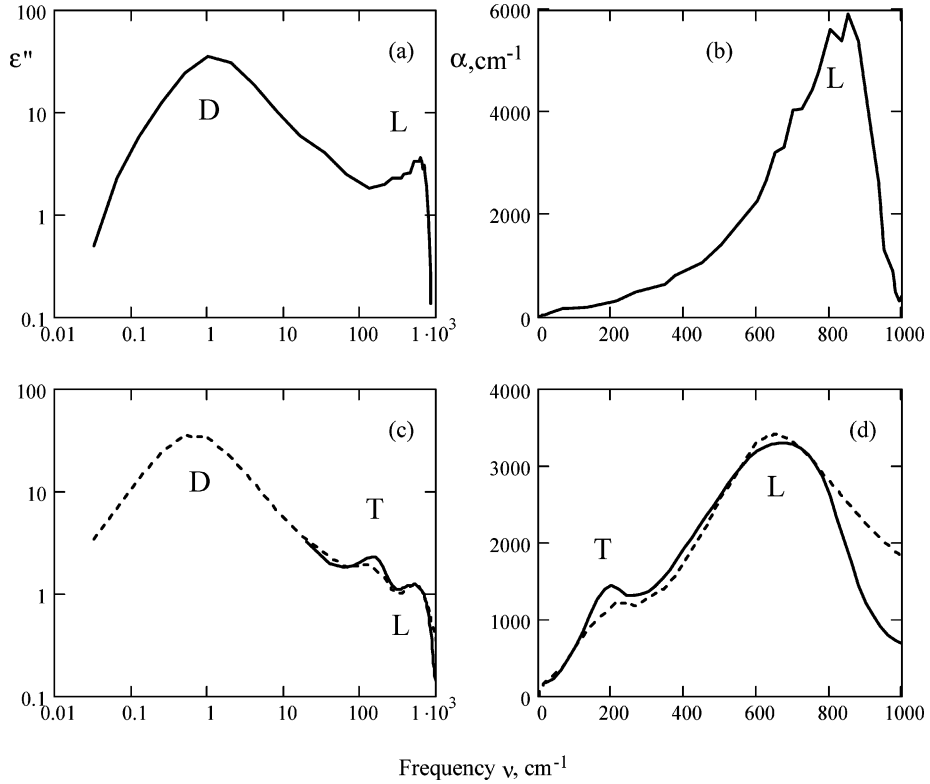

Figure 5. Spectra for water (H_2O) at 300 K: (a) loss spectrum, obtained by MD simulations; (b) absorption spectrum, obtained by MD simulations; (c) loss spectra, measured experimentally and in empirical relationships; and (d) absorption spectra. The experimental data from ref 14 are shown by the solid line. The spectra calculated by the empirical relation from ref 15 are shown by the dashed line. Symbols D, T, L refer, respectively, to Debye, translational, and librational band, respectively.

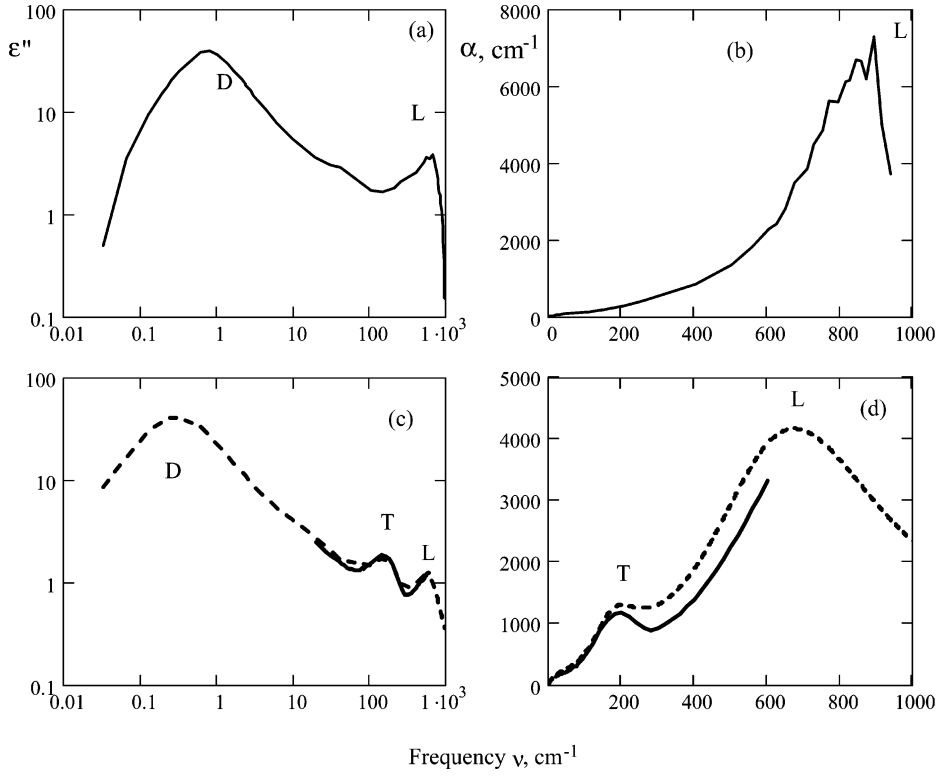

Figure 6. Same as Figure 5, but for a temperature of 273 K. Symbols D, T, and L refer, respectively, to Debye, translational, and librational bands.

In the MD-simulated Cole−Cole plot, shown in Figure 4a, we see, for the same reason, only one "curl", placed in the L-band. On the other hand, as shown in Figure 8b by the solid curve, the experiment[14] gives *two* curls, T and L, which are observed in the translational and librational bands, respectively. By analogy, the estimate, based on the empirical formulas,[15] also gives two such curls (shown by the dashed line in Figure 8). This problem is discussed below.

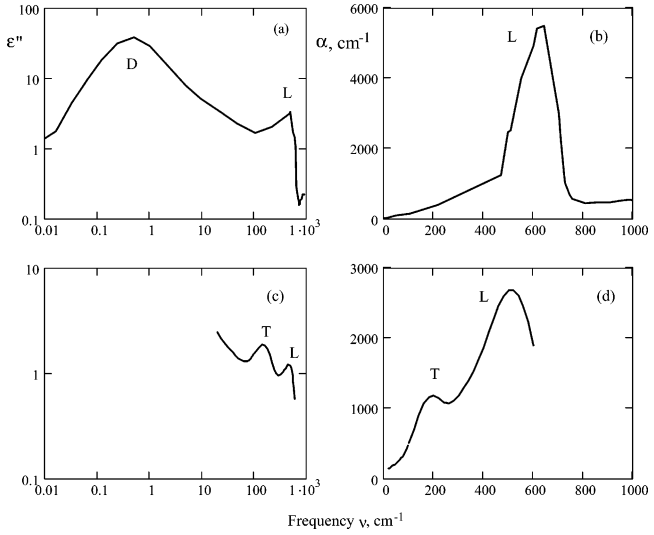

Figure 7. Same as Figure 6, but for heavy water (D_2O). Symbols D, T, and L refer, respectively, to Debye, translational, and librational bands.

4. Outline of the Analytical Approach

The results of the MD simulations are compared to those obtained by the analytical theory, in which the calculation of the ACF spectrum is based on application of the effective intermolecular potentials. The latter govern motion and the resulting dielectric response of interacting permanent (rigid) or flexible (nonrigid) dipoles.

The *two-fraction* composite model, described in ref 6 and, with more detail, in refs 7−10, is used. This model, which is comprised of the librational (LIB) and vibrational (VIB) fractions, permits calculation of the complex dielectric permittivity $\epsilon(\nu)$ and power absorption $\alpha(\nu)$ spectra of water, in the frequency range of 0−1000 cm^{-1}, and ice, in the frequency range of ∼10−1000 cm^{-1}. This LIB/VIB model allows analytical calculation of the ACF spectra determined by four molecular mechanisms, labeled here as a−d.

Mechanism a, which pertains to the LIB fraction, governs collision-interrupted reorientation (termed libration) of a permanent dipole in the intermolecular potential with a hatlike profile.

In the VIB fraction, the dielectric relaxation is treated in terms of a dimer of elastically vibrating H_2O or D_2O molecules, whose dielectric response is determined by the following three mechanisms: (b) harmonic vibration of a nonrigid dipole along the hydrogen bond (HB), (c) harmonic reorientation of permanent dipoles around the HB, and (d) non-harmonic vibration of two hydrogen-bonded water molecules transverse to the HB direction.

4.1. Mechanism a. Mechanism a reveals (1) a quasi-resonance dielectric response in the librational band (L-band) located at $\nu_{or} \approx 700$ cm^{-1} and (2) the nonresonance Debye relaxation band, with its loss peak ϵ'' located in the microwave region.

The L-band results from the almost free, but somewhat cooperative, reorientation of a water molecule, with the permanent dipole moment μ_{or}, during a lifetime τ_{or} in the hatlike potential well. The lifetime τ_{or} is of the order of fractions of a picosecond. The shape of the hat potential is characterized by a rather deep well, with the dimensionless (scaled by k_BT) depth of $u \approx 8$, and with a half-width of $\beta \approx 23°$ (where β is the libration amplitude). The bottom of the well is assumed to be flat. At higher temperatures, this profile is almost rectangular; at lower temperatures, it approaches a parabola. Note that the reorientation of a water dipole is nonlinear in nature. Consequently, the density of libration states is enriched with higher harmonics, especially at higher temperatures. Thus, in the FIR region, the librational-band shape is far from being Lorentzian.

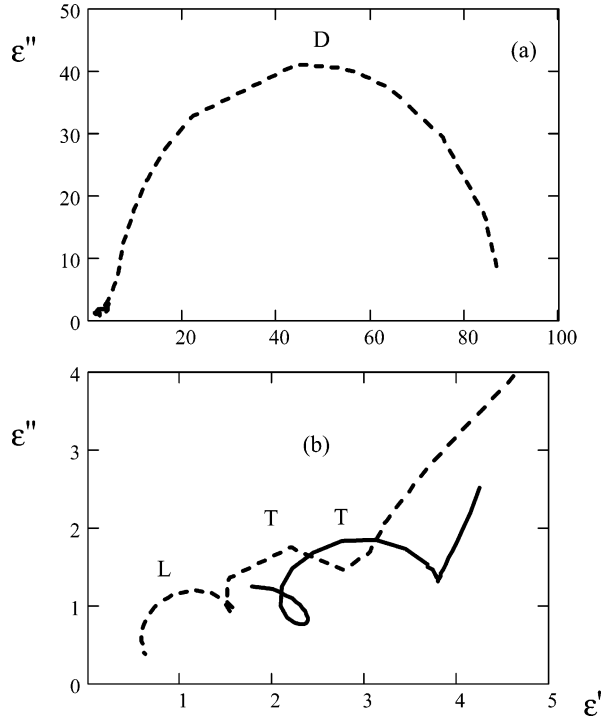

Figure 8. Cole−Cole diagrams (—) determined from the experimental data[14] and (- - -) estimated from the empirical formulas,[15] for water (H_2O) at 300 K. Symbols D, T, and L refer to the same designations as those given for Figures 5, 6, and 7.

The librational band is characterized by an isotopic shift of its peak located at ν_{or}. Because the librations are almost free, the frequency ν_{or} is determined by the moment of inertia I_{or}. Because $I_{or}(H_2O) \approx {}^1/_2 I_{or}(D_2O)$, the corresponding frequency is $\nu_{or}(H_2O) \approx \sqrt{2}\nu_{or}(D_2O)$.

We assign the VIB states to a water dimer, whose vibration, which is governed by mechanisms b, c, and d, is parametrized by three force constants: k, kc_{rot}, and $k_\perp$.

4.2. Mechanism b. Two oppositely charged ions form a nonrigid dipole $O^+-H\cdots O^-$ or $O^+-D\cdots O^-$ (other atoms can also be attached to these oxygen atoms). The concentration N_{vib} of *charged* dimer molecules comprises about one-third of the concentration N of water molecules ($N_{vib} \approx N/3$). This result follows from the parametrization of the model, if one assumes that the absolute value of the charge pertaining to each of the two dimer molecules comprises approximately the charge of an electron (other assumptions would appear to be unreasonable). One may assume that the charges appear due to the proton jump from one dimer molecule to the other. The recombination of these charges transforms the VIB fraction to the LIB fraction during the HB lifetime (about 0.1 ps).

A nonrigid dipole constituted by the dimer molecules executes longitudinal (viz. along the hydrogen bond) harmonic vibration, controlled by the force constant k. The latter is parametrized to reproduce the position of the loss peak ϵ_q'' in the translational band (T-band), centered at ∼180 cm^{-1}. Because the equation of motion for longitudinal vibration is linear, the band shape $\epsilon_q''(\nu)$ is close to Lorentzian. The peak frequency ν_q is almost independent of temperature, so that $\nu_q \approx 165$ cm^{-1}. At room temperature, however, the band shits to 190 cm^{-1}. This may

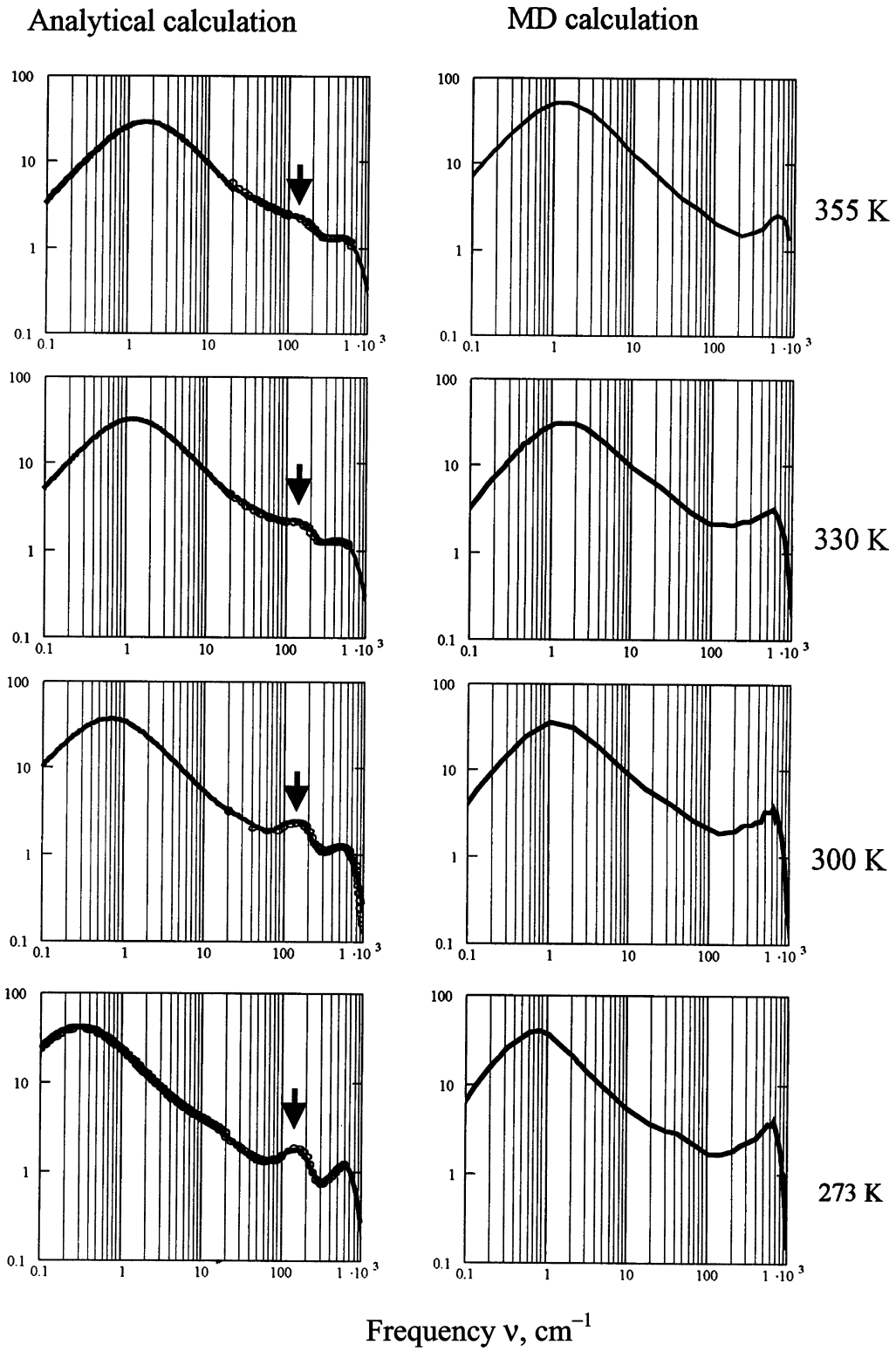

Figure 9. Evolution with temperature of the loss spectra of water (H_2O) obtained by analytical calculation (left column) and MD simulations (right column). Other explanations are given in the text.

be an indication of a certain change of structure[8] at ~300 K. An important feature of a hydrogen bond, determined by the quantum nature of interactions, is a rather weak isotopic dependence of the T-band. Thus, at room temperature (293 K), our analytical estimate of the shift $\Delta\nu_{\text{isotope}}$ between the loss maxima $\epsilon''_{q_{\max}}$ calculated for two specific loss curves, pertaining to mechanism b, is ~50 cm^{-1} (the loss maxima are located near 150 cm^{-1} for H_2O and at 200 cm^{-1} for D_2O). (We note that obtaining an accurate value of $\Delta\nu_{\text{isotope}}$ from the experimental data from ref 14 seems difficult.) On the other hand, analytical estimation, in terms of our theory, of the shift $\Delta\nu_{\text{isotope}}$ gives, for mechanism a (that is, for the librational band), a much larger value, viz. $\Delta\nu_{\text{isotope}} \approx 150$ cm^{-1} (the specific ϵ''_{or} maxima are placed at 450 cm^{-1} for D_2O and at ~600 cm^{-1} for H_2O).

The parametrization of the model shows that the mean elastic HB moment (μ_q) of a nonrigid elastic dipole is ~3 times larger than that of a permanent dipole (μ_{or}). This difference arises perhaps due to polarization of the hydrogen bond by dimer

charges. The lifetime is relatively short in water ($\tau_q \approx 0.08$ ps) and slowly increases as the temperature decreases.

4.3. Mechanism c. In a manner similar to that for mechanism b, mechanism c generates one Lorentz line (we indicate this as the V-band), with the peak centered at room temperature at $\sim$150 cm^{-1}. This position is determined by the rotary dimensionless force constant (c_{rot}). Note that the T- and V-bands overlap in water, but they are resolved in ice. The rotary-vibration lifetime (τ_μ) is similar to the longitudinal-vibration lifetime (τ_q). One may argue that both times are determined by the harmonic oscillation of a hydrogen bond.

4.4. Mechanism d. Mechanism d results as the dielectric response that is due to the vibration of two oppositely charged water molecules in the direction transverse to the equilibrium HB direction. This vibration, which is nonlinear in nature, is determined by the transverse force constant $k_\perp$ and by other dimer parameters. The peak transverse-vibration (TV) frequency ($\nu_\perp$) is centered near 30 cm^{-1}. The band shape of the TV loss frequency dependence ($\epsilon''_\perp(\nu)$) is not Lorentzian and is very damped (especially at low temperatures). This property could be attributed to collective oscillations of an ensemble of nonrigid dipoles.

5. Comparison of MD Simulations with Analytical Calculations

Here, we consider the temperature dependence of the loss spectra. In the left column of Figure 9, the solid lines show the loss spectrum of water (H_2O) calculated analytically for the temperatures of 273, 300, 330, and 355 K. The circles depict the experimental data.[12,14,15] As can be seen, the results obtained using the analytical theory (the model parameters are given in ref 8) are in a quantitative agreement with the experiment.

The MD calculations, as illustrated in the right column of Figure 9, give a rather qualitative agreement with the experimental data. *However, the employed MD calculation scheme, which has been briefly described previously, is incapable of describing the water spectra in the 200 cm^{-1} band.* This band, which is marked by an arrow in the left column, does not appear in the right column. Comparison with several other works shows that this drawback is generally characteristic for the currently used classical potential models that are used in MD simulations.

6. Concluding Remarks

Classical MD simulations, which include polarizable models, address the intensity of the translational mode by means of force fields, where each water molecule is polarized according to a local field, so that the induced polarization is intramolecular. In contrast, in the work by Sharma et al.,[1] it was shown, in terms of the first-principles quantum approach, that a tetrahedral coordination of oxygen atoms in the liquid is regarded as an assembly of electrons and nuclei and that the FIR spectra are dependent on concerted tetrahedral fluctuations of the hydrogen bonds. In this assembly, "the polarization effects" are dependent on the environment in a "strong *intermolecular* way", thus indicating the 200 cm^{-1} mode. The intramolecular polarization of a water molecule in the presence its (closest) neighbors may be seen in classical molecular dynamics (MD) simulations with a flexible model and/or effectively introduced polarization (for instance, through a polarizability tensor). Thus, we speculate that an indication of the translational mode (not necessarily at 200 cm^{-1}) may be observed in the spectra computed by the MD method with an appropriately parametrized flexible model for water.

In our analytical (classical) approach, which is based on intuitively introduced molecular potentials, depending on the appropriate force constants (regarded as fitted model parameters), the translational band is ascribed to interaction of adjacent charged molecules and, hence, generally is ascribed to the same origin, as is suggested by Sharma et al.[1] However, instead of considering an assembly of particles—as was done in the work of Sharma et al.[1]—we calculate the spectra generated (i) by *two* elastically vibrating charged HB molecules and (ii) by one polar molecule, almost freely librating in a certain intermolecular potential well. Then, as observed from the left column of Figure 9, it is possible to describe the translational band, as well as other bands of water in the range of 0−1000 cm^{-1}, in terms of the analytical theory that has been briefly reviewed previously. This theory connects a linear Lorentz-type dielectric response in the translation band (T-band) with fast vibration of two charged water molecules along the hydrogen bond (combined with harmonic reorientation of permanent dipoles about this bond) during a lifetime of $\sim$0.1 ps. Thus, this classical mechanism is in approximate correspondence with the quantum approach.[1]

Perhaps the main advantage of our analytical approach consists of the application of the *two-fraction* model, for which *two* features are characteristic:

(1) The main decrease in the permittivity constant $\epsilon'(\nu)$, with frequency ν, from the static value to $\epsilon_\infty \approx 3$, is determined by the motion of a polar water molecule, regarded as an *isolated* rigid dipole, noninteracting with other molecules and moving rather freely in a certain (hat) intermolecular potential.

(2) The T-band, which presents (in this context) a peak of our interest, is partially determined by an intermolecular vibration that is governed by the longitudinal force constant, whose value k is fitted to obtain the 200 cm^{-1} band.

One may suggest that (2) is *not* properly regarded in the current MD approach. However, we emphasize the inestimable advantage of the MD simulation method, in regard to its ability to *predict* the spectra (as well as many other important properties of investigated fluids) using *only* an intermolecular interaction potential. The analytical theory that has been used in this work is generally capable of parametrizing the model only ad hoc, using, to a greater or lesser extent, the experimentally obtained spectra. Therefore, it is reasonable to use both methods to calculate the water/ice spectra.

References and Notes

(1) Sharma, M.; Resta, R.; Car, R. *Phys. Rev. Lett.* **2005**, *95*, 187401.
(2) Car, R.; Parrinello, M. *Phys. Rev. Lett.* **1985**, *55*, 2471.
(3) Madden, P. A.; Impey, R. W. *Chem. Phys. Lett.* **1986**, *123*, 502.
(4) Silvestrelli, P. L.; Bernasconi, M.; Parrinello, M. *Chem. Phys. Lett.* **1997**, *277*, 478.
(5) Zasetsky, A. Yu.; Khalizov, A. F.; Sloan, J. J. *J. Chem. Phys.* **2004**, *121*, 6941.
(6) Gaiduk, V. I.; Crothers, D. S. F. *J. Phys. Chem. A* **2006**, *110*, 9361.
(7) Gaiduk, V. I.; Crothers, D. S. F. *J. Mol. Liquids* **2006**, *128*, 145.
(8) Gaiduk, V. I.; Crothers, D. S. F. *J. Mol. Struct.* **2006**, *798*, 75.
(9) Gaiduk, V. I.; Kutuza, B. G. *Opt. Spectrosc.* **2006**, *101*, 696. (Also in *Opt. Spektrosk.* **2006**, *101*, 744.)
(10) Tseitlin, B. M.; Gaiduk, V. I.; Nikitov, S. A. *J. Commun. Technol. Electron.* **2005**, *50*, 1002. (Also in *Radiotekh. Elektron. (Moscow, Russ. Fed.)* **2005**, *50*, 1085.)
(11) Bertie, J. E.; Lan, Z. D. *Appl. Spectr.* **1996**, *50*, 1047.
(12) Downing, H. D.; Williams, D. *J. Geophys. Res.* **1975**, *80*, 1656.
(13) Zasetsky, A. Yu.; Khalizov, A. F.; Earle, M. E.; Sloan, J. J. *J. Phys. Chem. A* **2005**, *109*, 2760.
(14) Zelsmann, H. R. *J. Mol. Struct.* **1995**, *350*, 95.
(15) Liebe, H. J.; Hufford, G. A.; Manabe, T. *Int. J. Infrared Millimeter Waves* **1991**, *12*, 659.
(16) Berendsen, H. J. C.; Grigera, J. R.; Straatsma, T. P. *J. Phys. Chem.* **1987**, *91*, 6269.

(17) Reddy, M. R.; Berkowitz, M. *Chem. Phys. Lett.* **1989**, *155*, 173.
(18) Lyubartsev, A. P.; Laaksonen, A. *Comput. Phys. Commun*. **2000**, *128*, 565.
(19) Nose, S. *Mol. Phys*. **1984**, *52*, 255.
(20) Ryckaert, J. P.; Ciccotti, G.; Berendsen, H. J. C. *J. Comput. Phys.* **1977**, *23*, 327.
(21) Caillol, J. M.; Levesque, D.; Weiss, J. J. *J. Chem. Phys.* **1986**, *85*, 6645.
(22) Warren, S. G. *Appl. Opt.* **1984**, *23*, 1206.
(23) Krishnamurthy, S.; Bansil, R.; Wiafeakenten, J. *J. Chem. Phys*. **1983**, *79*, 5863.